

Atomic layer deposition in preparing 2D-NS-photocatalysts for hydrogen generation-a comprehensive review

Ayesha Nazeer¹, Faisal Ahmad², Shamim Ahmad³

¹ToxAlliance LLC, Kennett Square, United States

²India Leaders for Social Sector, New Delhi, India

³Hamdard University, New Delhi, India

Article Info

Article history:

Received Oct 25, 2025

Revised Nov 29, 2025

Accepted Dec 14, 2025

Keywords:

2D nanosheets
Atomic layer deposition
Catalyst stability
Electrocatalysis
Hydrogen production
Photocatalysis
Solar-to-hydrogen efficiency

ABSTRACT

Hydrogen production through photocatalysis, electrocatalysis, and hydrolysis is a promising route to clean energy. However, persistent challenges—including low charge separation efficiency (<10% solar-to-hydrogen (STH)), limited catalyst stability (>1,000 h required), and reliance on noble metals—continue to hinder scalability. Two dimensional nanosheets (2D NS) have emerged as attractive platforms due to their tunable electronic structures and high surface activity, but conventional synthesis methods often fail to deliver uniform coatings, controlled defects, or stable heterojunctions. This limits systematic tuning of catalytic interfaces and prevents achieving both high efficiency and long-term durability in practical hydrogen production systems. This study highlights atomic layer deposition (ALD) as a precise strategy for engineering 2D NS photocatalysts. Representative systems such as COF/SnNb₂O₆ and NiO/CdS heterojunctions achieve 15.2% STH—2.3× higher than pristine SnNb₂O₆—via Z scheme charge transfer with I₃⁻/I⁻ mediators, reducing recombination by 78%. In electrocatalysis, ALD derived boron nanosheets deliver hydrogen evolution reaction (HER) overpotentials of 89 mV at 10 mA/cm², outperforming Pt/C (110 mV), while enabling NaBH₄ hydrolysis rates 4.5× faster than bulk catalysts. ALD strategies ensure scalable synthesis from abundant precursors, >95% durability over 2,000 cycles, and cost reductions of up to 60% compared with noble metal alternatives. By bridging gaps in efficiency, stability, and practicality, ALD engineered 2D nanosheets advance sustainable hydrogen production and accelerate pathways toward commercialization.

This is an open access article under the [CC BY-SA](#) license.



Corresponding Author:

Shamim Ahmad
Hamdard University
New Delhi, India
Email: drsahmad@email.com

1. INTRODUCTION

The transition toward a sustainable hydrogen economy has intensified research into efficient, low-carbon hydrogen production technologies. Among the available routes, photocatalytic and electrocatalytic water splitting, as well as chemical hydrolysis-based processes, are widely recognized for their environmental compatibility and long-term scalability. However, the practical implementation of these approaches is still constrained by low reaction kinetics, inefficient charge separation, and limited durability of catalytic materials.

Two-dimensional nanomaterials (2D-NMs) have alternately emerged as attractive platforms for hydrogen production owing to their ultrathin architectures, high surface-to-volume ratios, abundant exposed

active sites, and tunable electronic structures. These features are particularly beneficial for hydrogen evolution reaction (HER) and oxygen evolution reaction (OER), where rapid interfacial charge transport and minimized carrier recombination are essential. Consequently, a variety of 2D nanosheets, heterostructures, and hybrid architectures have been explored to enhance hydrogen generation efficiency through improved light absorption, catalytic activity, and charge-carrier dynamics.

Despite their intrinsic advantages, the performance of 2D-NM-based catalysts is strongly governed by surface defects, interfacial band alignment, cocatalyst dispersion, and structural uniformity. Conventional fabrication and modification techniques such as sol–gel synthesis, physical vapor deposition (PVD), and chemical vapor deposition (CVD) often lack the precision required for uniform coating and defect control on atomically thin 2D nanosheets. These limitations hinder systematic tuning of catalytic interfaces and restrict further performance enhancement.

In this context, atomic layer deposition (ALD) has emerged as a uniquely suited technique for engineering 2D-NM-based hydrogen production systems. Compared with sol–gel and CVD approaches, ALD provides atomic-level thickness control, excellent conformality, and precise composition modulation, even on high-aspect-ratio and ultrathin 2D substrates. Such capabilities enable controlled defect engineering, uniform cocatalyst loading, and the formation of well-defined heterojunctions, all of which are critical for promoting efficient charge separation, suppressing recombination losses, and improving hydrogen evolution efficiency.

Recent studies have demonstrated that ALD-engineered 2D heterostructures—such as metal/semiconductor interfaces, oxide-decorated nanosheets, and p–n junction architectures—exhibit significantly enhanced photocatalytic and electrocatalytic hydrogen production performance. By enabling precise control over interfacial chemistry and nanoscale architecture, ALD facilitates a deeper understanding of structure–property–activity relationships that is difficult to achieve using conventional deposition techniques.

Accordingly, this review critically examines the role of ALD in advancing hydrogen production using 2D nanosheet-based catalysts. The review is organized as follows: section 2 outlines the fundamental mechanisms of hydrogen production and key catalyst design requirements, section 3 introduces the principles and advantages of ALD in comparison with other deposition methods, section 4 discusses recent progress in ALD-modified 2D nanosheets for photocatalytic, electrocatalytic, and chemical hydrogen generation finally, section 5 highlights current challenges, future perspectives, and emerging research directions in ALD-engineered 2D nanomaterials for hydrogen production [1]–[8].

2. IDEAL FEATURES OF SOLAR PHOTOCATALYSTS FOR HYDROGEN GENERATION

Achieving high solar-to-hydrogen (STH) efficiency is the primary objective in photocatalytic hydrogen generation, requiring efficient light harvesting, rapid charge separation, strong redox capability, and long-term material stability. An ideal photocatalyst should preferably maximize solar absorption while minimizing charge-carrier recombination to enable HER and OER.

Efficient charge separation is a critical requirement, as photogenerated electron–hole recombination significantly limits hydrogen production efficiency. Among the various architectures developed to address this challenge, Z-scheme photocatalytic systems are particularly effective because they preserve strong redox potentials while promoting spatial separation of charge carriers. In a typical Z-scheme configuration, two semiconductors with staggered band structures are coupled either through a redox mediator (e.g., I_3^-/I^-) or via direct solid–solid interfaces. Upon light irradiation, photogenerated electrons from the oxidation photocatalyst recombine with holes from the reduction photocatalyst, leaving highly reducing electrons and strongly oxidizing holes spatially separated. This charge-transfer pathway suppresses bulk recombination and enhances overall photocatalytic efficiency.

Beyond charge separation, photostability and chemical robustness under prolonged illumination and aqueous environments are essential for sustained hydrogen production. Photocatalysts must resist photo corrosion, surface oxidation, and catalyst leaching, particularly during OER. In addition, broad solar absorption—extending into the visible and near-infrared regions—is necessary to utilize a larger fraction of the solar spectrum, while the use of earth-abundant and non-toxic elements is critical for scalability and environmental sustainability.

Although these features define the ideal photocatalyst, their realization is often limited by poor interfacial contact, uncontrolled defect densities, and non-uniform cocatalyst distribution in conventionally synthesized materials. ALD offers a unique pathway to overcome these challenges, particularly when combined with 2D nanosheets (2D-NSs). The atomic-scale thickness control and conformal coating capability of ALD enable precise tuning of band alignment, controlled defect engineering, and uniform cocatalyst deposition on ultrathin 2D substrates. Such attributes are especially advantageous for constructing Z-scheme heterostructures, where interfacial quality directly governs charge-transfer efficiency.

ALD-modified 2D nanosheets thus provide an effective platform to enhance key photocatalyst features, including interfacial stability, carrier lifetime, and redox efficiency. By enabling rational interface design and reproducible structural control, ALD bridges the gap between ideal photocatalyst requirements and experimentally realizable hydrogen production systems [9]-[16].

3. RECENT R&D HIGHLIGHTS

The AZ-scheme based photocatalytic system with separate H₂ and O₂ evolution chambers using dipolar membranes, has achieved efficient overall water splitting while suppressing reverse reactions [10]. Advances in organic photocatalysts have examined the possibilities of improving the light absorption and charge transfer properties, making them promising candidates for solar-driven water splitting processes [9]. Based on the latest research studies, the ideal features of a solar photocatalyst for hydrogen generation from water splitting are thus enlisted below. Fu *et al.* [10], noted some useful observations in this context of solar to hydrogen efficiency enhancements as listed here.

In a recent study, an STH efficiency of 2.47% was reported in laboratory conditions from the halide perovskite photocatalysts like MoSe₂-loaded CH(NH₂)₂PbBr_{3-x}I_x, which is notable figure for practical applications. For efficient charge separation it is essential to minimize recombination of photogenerated electron-hole pairs. A Z-scheme system, which uses redox mediator like I₃⁻/I⁻, has been found facilitating efficient electron transfer and suppressing reverse reactions, enhancing overall efficiency. For minimising photocatalyst degradation under prolonged exposure to sunlight and water, materials like NiFe-layered double hydroxide (LDH) modified BiVO₄ are known to exhibit enhanced stability during water oxidation processes.

In the context of absorbing a wide spectrum of solar light, including visible and near-infrared wavelengths, organic photocatalysts and halide perovskites are observed to capture more photons across the solar spectrum [9]. To avoid recombination of hydrogen and oxygen, systems must separate the evolution chambers for H₂ and O₂ using dipolar membranes or similar technologies. This separation ensures safety and improves efficiency. Scalable designs are essential for practical applications. Recent advancements include panel reactor modules capable of tandem scaling up for large-area applications, as demonstrated in outdoor setups with average STH efficiencies of 1.21% under natural sunlight. For the materials used ultimately be abundant and inexpensive to ensure economic viability. For example, BiVO₄ films combined with commercial carbon cloth provide cost-effective solutions for water oxidation. Besides, integration with effective redox mediators like I₃⁻/I⁻ has demonstrated the enhanced efficiency of Z-scheme systems to facilitate electron transfer between HER and OER chambers [9]. The system should ultimately avoid using toxic or rare materials, ensuring eco-friendliness and sustainability in production and operation.

Z-scheme photocatalytic systems are noted to separate H₂ and O₂ evolution in respective chambers using dipolar membranes, achieving efficient overall water splitting while suppressing reverse reactions [10]. Advances in organic photocatalysts have improved light absorption and charge transfer properties, making them promising candidates for solar-driven water splitting [9]. Outdoor setups with panel reactors have demonstrated the feasibility of scaling up solar-driven systems while maintaining reasonable efficiencies under natural sunlight conditions [10]. By incorporating these features in the materials used appropriately, solar photocatalysts can achieve higher efficiencies, stability, and scalability, paving the way for sustainable hydrogen production through water splitting technologies [9], [10], [17]-[32].

3.1. Near ideal photocatalytic material—achievable by material design and synthesis

The first parameter to check in this context to examine the semiconductor's bandgap for achieving optimized to absorb a wide range of solar light, typically in the visible spectrum, enhancing photocatalytic efficiency [18], [20]. Incorporating materials to enhance light absorption deploying materials like plasmonic metals or dyes, might be attempted to improve photocatalytic activity [20], [31]. Designing nanostructured photocatalysts becomes imperative to increase the surface area, facilitating better charge separation and transfer [25], [31].

Implementing a Z-scheme mechanism another possibility for efficient electron transfer between different components, enhancing overall water splitting efficiency [10]. Choosing stable materials like sodium-tantalate or graphitic carbon nitride is yet another route that ensures long-term photocatalytic activity [9], [31]. Coating or modifying the surface can be explored for protecting the photocatalyst from degradation under solar radiation [20].

Doping with metals like Pt, Au, or Ni can significantly enhance the catalytic activity for hydrogen evolution. Creating composites with different materials (e.g., Ce₃O₄@C/TiO₂) can improve photocatalytic performance [25].

Developing scalable systems with separate reaction chambers for hydrogen and oxygen evolution must be explored with improved efficiency and safety as in case of solar photovoltaic panels [10]. Using cost-effective materials and designs can make large-scale hydrogen production more feasible as expected from the recent studies [18].

These above-mentioned experimental observations do indicate the feasibility of how to optimise the material design, and synthesis for significantly enhancing the efficiency and practicality of photocatalysts for solar-driven hydrogen production. The design of nanomaterials for solar-driven hydrogen generation involves balancing light absorption, charge dynamics, and catalytic activity. Recent advancements in 0D, 1D, and 2D nanomaterials and their composites reveal distinct advantages do indicate towards this possibility as described below. Before proceeding further in this exploration, it will be worthwhile to examine the basic features of lower dimensional nanomaterials (e.g., 0,1, and 2D-Nanomaterials and their combinations) as highlighted briefly in Table 1.

Table 1. Comparison of nanomaterial dimensions for photocatalytic H₂ generation

Dimension	Strengths	Limitations	Key advances
0-D	High surface-to-volume ratio, abundant active sites, tunable optoelectronic properties [24].	Poor charge carrier transport, and risk of aggregation limit the light-harvesting efficiency.	Pd-NPs cocatalysts enhance H ₂ evolution rates in 0-D/1-D/2-D composites (e.g., Pd/TiO ₂ /g-C ₃ N ₄ achieves 11.62 mmol/h/g) [21].
1-D	Fast axial charge transport, reduced recombination, and improved structural stability.	Limited surface area compared to 2D materials, challenges in heterojunction design.	TiO ₂ nanofibers (1-D) in 1-D/2-D heterostructures with g-C ₃ N ₄ improve charge separation and visible-light response [21].
2-D	Large reactive surface area, short charge diffusion paths, and flexible heterojunction designs [24].	Lower charge mobility compared to 1-D materials, and scalability challenges.	g-C ₃ N ₄ nanosheets enable Z-scheme heterojunctions for efficient electron-hole separation [21], [24].

While examining the possibility of realizing optimal nanostructured material, it is obvious to attempt various combinations of 0,1, and 2D materials and see the possible improvements if any. This exercise offered the following observations. Band alignment between TiO₂ (1-D) and g-C₃N₄ (2-D) creates a type-II heterojunction, directing electrons to TiO₂ and holes to g-C₃N₄ [21]. 2-D-g-C₃N₄ extends visible-light absorption, while 1D-TiO₂ ensures rapid electron transport [21]. 0-D-Cocatalysts (e.g., Pd-NPs) provide active sites for proton reduction and suppress recombination via Schottky junctions [21]. Hydrophilic 0-D polymer NPs with proton channels mimic natural photosynthesis with improved H₂ yield [9], [10], [17]-[32].

4. MATERIAL DESIGN STRATEGIES

Efficient solar-driven hydrogen production requires precise regulation of semiconductor band structure, surface defects, and interfacial charge-transfer pathways. While conventional nanomaterial synthesis techniques enable the formation of 0D, 1D, and 2D architectures, their limited control over surface chemistry and interface uniformity often restricts photocatalytic performance. In this context, ALD has emerged as a critical post-synthetic strategy for engineering 2D photocatalysts with atomic-scale precision.

Multidimensional architectures, particularly 1D/2D and 0D/1D/2D heterostructures, offer synergistic advantages by combining efficient charge transport, high surface activity, and enhanced catalytic functionality. However, the performance of these systems is predominantly governed by defect density and interfacial quality. ALD addresses these challenges by enabling controlled surface passivation, band alignment engineering, and uniform cocatalyst deposition on ultrathin 2D nanosheets.

4.1. Conventional synthesis routes: scope and limitations

Established methods such as sol-gel processing, hydrothermal synthesis, CVD, electrospinning, and mechanical or chemical exfoliation are widely used to prepare nanomaterials with tailored morphology and crystallinity. However, these approaches often result in non-uniform surface states, uncontrolled defect concentrations, and weak interfacial contact, particularly for atomically thin 2D materials. Consequently, post-synthetic surface engineering is essential to achieve high photocatalytic efficiency, as summarized in Tables 2-7, which lists representative materials employed for photocatalytic hydrogen production.

Table 2. Titanium dioxide photocatalyst

Photocatalyst	H ₂ production (μM/h/g)	Reaction conditions
Pt single atoms on a defective TiO ₂ (Pt/def-TiO ₂). Ru on the polygonal TiO ₂ sphere. Ru single atoms (SAs) into N-doped TiO ₂ /C carrier (Ru-SAs@N-TC) derived from metal-organic frameworks (MOF) of NH ₂ -MIL-125.	52,720 7.2 100	CH ₃ OH as sacrificial electron donor. 300 W Xe lamp; CH ₃ OH (aq.). 300 W Xe lamp (λ =320–780 nm); 20 mg of catalyst dispersed in 100 mL of H ₂ O: MeOH solution (v/v =4:1).
Ag/TiO ₂ .	470	254 nm wavelength of UV light catalyst concentration of 20 mg/L. 50 mL of solution without sacrificial agent.
Ga-doped TiO ₂ .	5,722	Side-irradiation by a 150 W xenon arc lamp equipped with an aqueous CuSO ₄ filter (310 nm < λ < 625 nm). 3 mg of the catalyst suspended in 3 mL of aqueous methanol solution (20 vol.%).
Co-, Ni-, and Cu-doped TiO ₂ .	8,470 (Cu) 3,390 (Ni)	450 W Hg lamp. 10 mg photocatalyst in solution with 50% MeOH as a sacrificial electron donor.
Mesoporous core-shell CdS@TiO ₂ with Pt.	68,000	10 mg photocatalyst dispersed in 50 mL of an aqueous solution of sacrificial reagent (0.1 M Na ₂ S+0.02 M Na ₂ SO ₃).

Table 3. Graphitic carbon nitride photocatalyst

Materials	H ₂ production (μM/h/g)	Reaction conditions
UNiMOF/g-C ₃ N ₄ . Heterostructure with 2D- nickel metal organic framework (UNiMOF) nanoflakes and 2D g-C ₃ N ₄ nanoflakes.	20.03	300 W Xe lamp with a 420 nm filter. 50 mg of catalyst dispersed in 90 mL of H ₂ O mixed with 10 mL of triethanolamine (TEOA).
NiAl-LDH/gC ₃ N ₄ . gC ₃ N ₄ coupled NiAl LDH nanocomposite.	3,170	Stimulated light irradiation (300 mW/cm ²). 15 mg of photocatalyst suspended in 50 mL of solution containing 45 mL H ₂ O and 5 mL TEOA as a sacrificial reagent.
Pd/g-CN. Pd single atoms in the space of adjacent g-CN layers and anchored Pd atoms on the surface of g-CN.	6,688	Solar simulator as a light source; 50 mg of the photocatalyst dispersed in 80 mL of water and TEOA solution (v/v=9:1).
Co SAs on carbonitride, and creating an active single Co ₁ -N ₄ site on g-C ₃ N ₄ .	10,800	Simulated solar irradiation (λ ≥300 nm). Triethanolamine (TEOA) as the sacrificial electron donor.
Co ₁ -P ₄ site confined on g-C ₃ N ₄ NSS.	410,300	Simulated solar irradiation. 20 mg of photocatalyst without sacrificial e- donor.
Co-N-C/g-C ₃ N ₄ . Isolated cobalt (Co) SAs synthesized and immobilized on a porous nitrogen-doped carbon support.	1,180,000	LED light source (λ =420±10 nm). 2 mg of the catalyst suspended in an aqueous solution with 10 vol.% TEOA as the sacrificial electron donor.

Table 4. Perovskite-based photocatalysts

Materials	H ₂ production (μM/h/g)	Reaction conditions
Ag/LaNaTaO ₃ .	329.5	500 W Xe lamp (λ >320 nm). 50 mg of catalyst suspended in 200 mL of 10 vol.% glycerol.
Ag/La _{0.02} Na _{0.98} TaO ₃ .	330	UV 500 W Xe lamp (λ >320 nm). 50 mg of the photocatalyst dispersed in 200 mL of a glycerol solution (10 vol.%).
AgInS ₂ QDs/Bi ₂ WO ₆ composite.	611	1000 W X lamp. 0.1 g of the photocatalyst dispersed in an 80 mL aqueous solution containing 1 M NaOH, 0.1 M Na ₂ S*9H ₂ O, and 0.5 M Na ₂ SO ₃ .
Ag/KTaO ₃ .	2,072	450W Xe-Hg UV lamp. 10 mg of the photocatalyst dispersed in 38 mL water and 12 mL methanol as a sacrificial agent.
CdS/NiWO ₄ /CoP. Composite catalyst with CoP-NPs co-catalyst modifying CdS/NiWO ₄ p-n heterojunction.	47,700	Visible light irradiation (λ >400 nm). 0.01 g of catalysts dispersed in 30 mL of 10% lactic acid solution.

Table 5. MOFs-based photocatalysts

Materials	H ₂ production (μM/h/g)	Reaction conditions
TiO ₂ -Ti ₃ C ₂ -CoS _x . TiO ₂ nanocrystal photocatalyst confined by ZIF-67-templated porous CoS _x , with conductive Ti ₃ C ₂ .	9,500	UV-visible light irradiation, methanol as the sacrificial agent.
TiO ₂ /CuO heterostructure derived from mixed-phase MOFs based on Ti and Cu metal nodes (MIL-125, Cu-BDC, MIL-125 xCu).	19,036	450 nm LED lamp. 0.2 mg of metal oxide catalysts mixed with [Ru(bpy) ₃] Cl ₂ ·6H ₂ O (2 mg), acetonitrile (3.8 mL), and TEOA (0.2 mL).
TiO ₂ /Co ₃ O ₄ /Ni. Highly porous ternary photocatalyst constructed from a heterometal-organic framework (H-MOF) template (ZIF-67@MIL-125).	27,000	Under UV-visible, light, and methanol solution.

Table 6. COFs-based photocatalysts

Materials	H ₂ production (μM/h/g)	Reaction conditions
CYANO-COF-cyano-containing COF with ketene-cyano (D-A) pair.	1,217	300 W Xe lamp ($\lambda > 420$ nm); 20 mg catalyst suspended in 100 mL water, 1 wt.% Pt (co-catalyst), and 10 mmol ascorbic acid (sacrificial agent).
Vinylene-linked 2D-COFs containing benzobisthiazoles units.	15,100	300 W Xe lamp ($\lambda > 420$ nm). COFs materials suspended in 0.1 M ascorbic acid solution.
Tp-nC/BPy ²⁺ -COFs. Cyclic diquats integrated into a 2,2'-bipyridine-based COF through a post-quaternization reaction.	34,600	Visible light irradiation ($\lambda > 420$ nm) in the presence of ascorbic acid (sacrificial donor) and Pt (co-catalyst).

Table 7. Miscellaneous

Materials	H ₂ production (μM/h/g)	Reaction conditions
CdS/Co _{1-x} S HHNSs. Sugar-gourd-shaped hollow hetero-nanostructure, Co _{1-x} S hollow polyhedrons skewered on CdS nanowires.	13,480	300 W Xe lamp ($\lambda > 420$ nm). 20 mg of photocatalysts dispersed in 100 mL of aqueous solution containing 20% lactic acid as the sacrificial agent.
Ag/ZnO/CeO ₂ .	18,345	300 W Xe lamp irradiation. 5 mg of the catalyst dispersed in 40 mL of water and 10 mL of glycerol.
ZCS QDs. Ni atomically dispersed in zinc sphalerite cadmium-zinc sulphide QDs.	18,870	300 W Xe lamp with a UV-cut-off filter ($\lambda \geq 420$ nm). 10 mg of photocatalyst suspended in a mixed solution of water and TEOA (20 vol.%) as a sacrificial reagent.
CuIn-CdS. Quantum dot level Cu and In co-doped CdS.	105,440	300 W Xe lamp as simulated solar light source (320–780 nm). 10 mg of photocatalyst dispersed in 25 mL of aqueous solution with 0.35 M of sodium sulphide and 0.25 M of sodium sulphite as sacrificial agent, and with 0.1 mL of H ₂ PtCl ₆ solution (1 mg/mL) as co-catalyst.

4.2. Role of atomic layer deposition in engineering 2D photocatalysts

ALD enables the conformal deposition of ultrathin functional layers with angstrom-level thickness control, making it uniquely suitable for modifying 2D nanosheets. Its key contributions include:

- Defect passivation: ALD-grown oxides suppress surface recombination centers and extend charge-carrier lifetimes.
- Band alignment control: precisely tuned ALD layers facilitate efficient charge separation in type-II and Z-scheme heterostructures.
- Cocatalyst regulation: uniformly dispersed metal and metal oxide cocatalysts maximize active-site utilization.
- Interfacial stabilization: conformal coatings protect 2D materials from photo corrosion and chemical degradation.

These features make ALD particularly effective for constructing stable, high-efficiency photocatalytic systems.

4.3. Recent progress and remaining challenges

ALD-modified 2D nanosheets have demonstrated enhanced hydrogen evolution activity, improved stability, and superior reproducibility compared with conventionally prepared catalysts. Representative systems are summarized in Table 8. Despite these advances, challenges related to scalability, precursor cost, and deposition throughput remain. Emerging approaches such as spatial ALD and roll-to-roll processing are expected to improve industrial viability [11]-[13], [33]-[61].

Table 8. Representative ALD-Modified 2D photocatalysts for hydrogen production

2D material	ALD	Key function	Performance enhancement
TiO ₂ - NSs	Al ₂ O ₃	Defect passivation	↓ Recombination, ↑ H ₂ yield
MoS ₂	TiO ₂	Band alignment	↑ Charge separation
g-C ₃ N ₄	Pt	HER cocatalyst	↑ H ₂ evolution rate
Graphene/rGO	NiO	Hole extraction	Enhanced stability
CdS - NSs	ZnO	Surface protection	Reduced photo corrosion

5. ATOMIC LAYER DEPOSITION IN PHOTOCHEMICAL WATER SPLITTING

Photoelectrochemical (PEC) water splitting requires semiconductor photoelectrodes with suitable band-edge alignment, efficient charge separation, fast interfacial charge-transfer kinetics, and long-term chemical stability in aqueous electrolytes. Although these requirements are well established, their simultaneous realization in a single material system remains challenging. ALD has emerged as a powerful enabling technique to address these limitations by offering angstrom-level thickness control, conformal coating of complex nanostructures, and precise interfacial engineering.

The role of ultrathin ALD layers at the semiconductor/electrolyte interface can be demonstrated using representative photoanode materials such as Fe_2O_3 , TiO_2 , and WO_3 . In these systems, ALD layers modify band bending, passivate surface states, suppress interfacial recombination, and improve charge-transfer kinetics without significantly impeding light absorption when optimized thicknesses are employed.

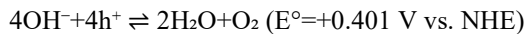
From a thermodynamic perspective, efficient PEC operation requires that the conduction and valence band edges of the photoelectrode straddle the H^+/H_2 and $\text{O}_2/\text{H}_2\text{O}$ redox potentials (1.23 V vs. NHE). In practice, kinetic overpotentials and surface recombination losses necessitate additional interfacial optimization. ALD addresses this gap by enabling controlled deposition of ultrathin oxides (e.g., Al_2O_3 , TiO_2 , and NiO_x), which tune surface energetics and stabilize the semiconductor under operating conditions.

In alkaline electrolytes, the relevant half-reactions are:

- Hydrogen evolution:



- Oxygen evolution:



The practical performance of PEC electrodes is therefore governed not only by bulk light absorption but also by interfacial charge-transfer kinetics and corrosion resistance—both of which are strongly influenced by ALD-derived surface modifications [60].

5.1. Protective atomic layer deposition coatings on photoelectrodes

Many high-absorption semiconductors (e.g., Si, Cu_2O , ZnO , and sulfide-based absorbers) suffer from severe photo-corrosion under PEC operating conditions. ALD-grown protective coatings provide an effective strategy to decouple light absorption from electrochemical stability. Ultrathin TiO_2 or Al_2O_3 layers deposited by ALD act as chemically robust barriers while remaining sufficiently thin (<5-10 nm) to allow tunneling-assisted charge transfer.

For example, ALD-deposited Al_2O_3 on hematite photoanodes has been shown to passivate surface trap states, resulting in anodic shifts of the photocurrent onset potential by ~80–100 mV and improved photocurrent stability under prolonged illumination. The conformality of ALD coatings ensures uniform protection even on high-aspect-ratio nanostructures, minimizing parasitic light absorption and preserving photon-to-current conversion efficiency.

5.2. Atomic layer deposition-engineered metal oxide photoelectrodes

Among ALD-grown metal oxides, Fe_2O_3 , TiO_2 , and WO_3 have received the most attention for PEC water splitting due to their chemical stability and earth abundance. However, their intrinsic limitations—short carrier diffusion lengths (Fe_2O_3), wide bandgaps (TiO_2), and suboptimal band-edge alignment (WO_3)—necessitate interfacial and bulk modification. ALD enables systematic tuning of these properties. Ti-doping of hematite via ALD, for instance, has been shown to increase hole mobility and lifetime, leading to enhanced photocurrent densities and more favorable onset potentials. Similarly, ultrathin ALD-grown Al_2O_3 layers on Fe_2O_3 suppress surface recombination by passivating defect states, while subsequent catalyst deposition (e.g., Co-Pt, IrO_2) accelerates oxygen evolution kinetics and reduces overpotentials. For WO_3 photoanodes, ALD-grown Al_2O_3 or TiO_2 overlayers have been reported to passivate surface states and improve Faradaic efficiency by mitigating electron trapping. In heterostructured architectures, ALD facilitates the formation of well-defined junctions that promote directional charge transport and reduce bulk recombination losses. These representative advances are summarized in Table 9, which lists ALD-modified photoelectrodes and their performance enhancements.

Table 9. ALD-modified photoelectrodes

Photoelectrode	Ald	Interfacial modification	Photocurrent density	Onset potential	Stability	Conditions	References
BiVO ₄ /NiCo ₂ O ₄ (p-n HJ)	TiO ₂	Surface defect passivation; enhanced hole injection	3.6 at 1.23 V	Not explicitly given	~95% of initial photocurrent retained after 10 h	pH ~7), sunlight	[61]
BiVO ₄ (single semiconductor)	TiO ₂	Passivation of surface electron-trap states	1.1 at 1.23 V (vs 0.64 baseline; +72%)	—	—	Phosphate buffer	[62]
Bi ₂ S ₃ /NiS (p-n H-J)	NiFeOx (OER cocatalyst) + TiO ₂	NiFeOx: water-oxidation cocatalyst; TiO ₂ : passivation	33.3 at 1.23 V	—	No degradation under continuous operation @ 1.23 V	Seawater AM1.5G	[42]
n-Si/BiVO ₄ (tandem integrated PEC)	Al ₂ O ₃ + ITO	Band-offset engineering and defect passivation	—	Shifted cathodically by 0.51 V (onset -0.36 vs +0.15 V _{RHE})	~1000 h (unbiased water splitting, STH ~0.62%)	Coupled to H ₂ -evolving cathode	[44]
Cu ₂ O (p-type photocathode)	Ga ₂ O ₃ + ZnGeO _x (oxide) + TiO ₂	Dual-buffer layers improve photovoltage (band alignment)	~5 (saturated at 0 V bias)	0.91 → 1.07 V (RHE) with dual buffers	Stable ~10 h @ 0 V _{RHE}	pH 5 phosphate-sulfate	[38]
WO ₃ (mesoporous) (heterojunction)	Fe ₂ O ₃	Core-shell H-J: enhanced light absorption, reduced recombination	~4.0 at 1.6 V (RHE)	≈1.2 V (RHE; not explicitly reported)	—	0.1 M HClO ₄ (acidic)	[59]

Notes: all photocurrent and onset values are reported under standard 1-sun (AM 1.5G) illumination unless noted. In each case the ALD overlayer (oxide-based unless stated) altered the interface to improve PEC metrics (e.g., by passivating traps or adding catalytic sites). The cited studies explicitly link the ALD-layer chemistry and function to the measured gains in photocurrent, onset potential shifts, or stability improvements.

5.3. Challenges and outlook

Despite its demonstrated benefits, the large-scale implementation of ALD in PEC systems faces several challenges. These include relatively low deposition rates, scalability to large-area substrates, and the use of metal-organic precursors that may pose cost or toxicity concerns. Recent advances (2023–2025) in spatial ALD, atmospheric-pressure ALD, and precursor chemistry are actively addressing these limitations and improving process throughput.

Overall, ALD has evolved from a protective coating technique to a versatile interfacial engineering tool for PEC water splitting. By enabling precise control over surface energetics, charge-transfer pathways, and chemical stability, ALD plays a critical role in bridging the gap between fundamental photoelectrode materials and practically viable solar hydrogen production systems.

5.3.1. Conformal atomic layer deposition overlayer improves hematite photoelectrochemical performance

Wang *et al.* [61] demonstrated that a conformal ultrathin TiO₂ overlayer deposited by ALD on hematite nanorod photoanodes can be precisely controlled in thickness to optimize interface charge transfer and overall water splitting efficiency under visible and UV illumination. This work systematically links ALD thickness to interfacial charge dynamics and enhanced PEC output.

5.3.2. Plasma-enhanced atomic layer deposition for thickness-controlled α -Fe₂O₃

A plasma-enhanced ALD (PEALD) process was developed for uniform α -Fe₂O₃ thin films, showing that ultrathin, conformal Fe₂O₃ deposited by ALD on high-aspect-ratio arrays enables improved PEC water splitting performance through optimized morphology and charge transport [62].

5.3.3. Atomic layer deposition -deposited TiO₂ passivation on Cu₂O photocathodes

Recent ALD work reported TiO₂ passivation layers on Cu₂O photocathodes, mitigating photo corrosion and improving kinetics. In these systems, ALD-grown TiO₂ significantly enhanced photocurrent density (~3.7 mA cm⁻²) and PEC conversion efficiency, underscoring the value of ALD for surface

stabilization and charge management [63]. Table 9 compares the performance of various cathodes using ALD materials.

6. PROSPECTS AND CHALLENGES

ALD is a versatile technique for fabricating high-quality thin films with precise control over thickness and composition. Despite its relatively recent development in the mid-1970s, ALD has gained significant attention in various fields, including PEC water splitting. In PEC applications, ALD can be employed for both the synthesis of the active material and the protection of photoelectrodes. The latter is particularly crucial, as the harsh operating environment of PEC cells can lead to corrosion and degradation of the electrode surface.

The electrolyte used in PEC cells can be corrosive and highly reactive, accelerating the deterioration of the electrode material. Additionally, the photogenerated charge carriers can induce photo-corrosion, further compromising the device's performance. The by-products produced during water splitting can also contribute to corrosion, hindering the long-term stability and efficiency of PEC cells. ALD-based protective layers can play a crucial role in mitigating these challenges. By passivating the electrode surface, ALD can prevent corrosion and enhance the device's lifetime. However, it is essential to select an appropriate material for the protective layer that allows for efficient electron transfer while retarding corrosion reactions.

The design and engineering of new materials for efficient PEC devices is another area where ALD can contribute significantly. ALD can be used to grow thin films of metal oxides, heterostructures (p-n junctions), and various catalysts, providing opportunities for systematic modification and improvement of existing technologies.

ALD-deposited overlayers can influence the semiconductor surface environment and modify the performance of PEC devices. These modifications can include a shift in the onset potential, either by reducing the catalytic overpotential or reducing the surface recombination rate. The passivation layer can also increase the photovoltage, leading to a cathodic shift of the onset potential. Extensively studied metal oxides for overlayer coatings include ZnO , Al_2O_3 , and TiO_2 . However, electron transfer via tunneling decreases exponentially with increasing layer thickness.

The future for ALD in the synthesis and modification of PEC devices is promising. Progress can be expected in areas such as metal particle ALD as catalysts, precise bandgap tuning through the deposition of nanolaminates, and focused doping of metal oxides. These advancements will contribute to the development of more efficient and durable PEC devices for sustainable energy applications. Solar-driven water splitting presents a promising avenue for establishing a sustainable and carbon-free renewable energy source. Numerous earth-abundant materials have been synthesized and evaluated as photoanodes or photocathodes for PEC devices. However, their implementation in efficient and long-lasting devices remains challenging due to several limitations.

Effective PEC materials must possess a combination of desirable properties, including chemical stability, suitable light absorption, high charge-carrier collection efficiency, low reaction overpotential, large photovoltage, and economic feasibility. To date, semiconductor-based photoactive materials have not achieved practical viability, primarily due to the lack of suitable candidates or stability issues under harsh operating conditions. ALD offers a promising approach to address these challenges and enhance the efficiency of photoanode materials. By precisely controlling the deposition of thin films at the atomic level, ALD can improve light absorption, charge carrier separation, and stability, leading to more efficient and durable PEC devices.

7. CONCLUSION

ALD is a highly promising technique for addressing persistent challenges in sustainable hydrogen production, particularly in enhancing the efficiency and durability of photocatalytic and electrocatalytic systems. The ability of ALD to produce ultra-thin, highly conformal films with atomic-scale precision is uniquely suited for engineering the complex 2D nanomaterial heterojunctions and active surfaces required for next-generation catalysts. The key benefits demonstrated include significant improvements in charge separation efficiency, notable reductions in reaction overpotentials compared to traditional catalysts like Pt/C, and superior long-term material stability by mitigating corrosion and sintering issues. Despite its potential, challenges remain regarding the inherent high cost, slow deposition rates, and the need for more efficient precursor utilization, particularly in scaling up from lab settings to commercial, industrial applications. Future research should focus on optimizing reactor designs for large-scale production, developing new, cost-effective precursors, and leveraging computational modeling to overcome these limitations and fully realize the potential of ALD-engineered materials in a future hydrogen economy.

REFERENCES

- [1] M. Cai *et al.*, “2D semiconductor nanosheets for solar photocatalysis,” *EcoEnergy*, vol. 1, no. 2, pp. 248–295, 2023, doi: 10.1002/ece2.16.
- [2] C. Feng, Z. P. Wu, K. W. Huang, J. Ye, and H. Zhang, “Surface Modification of 2D Photocatalysts for Solar Energy Conversion,” *Advanced Materials*, vol. 34, no. 23, pp. 1–33, 2022, doi: 10.1002/adma.202200180.
- [3] M. Li, H. Zhang, Z. Zhao, P. Wang, Y. Li, and S. Zhan, “Inorganic Ultrathin 2D Photocatalysts: Modulation Strategies and Environmental/Energy Applications,” *Accounts of Materials Research*, vol. 4, no. 1, pp. 4–15, 2023, doi: 10.1021/accountsmr.2c00172.
- [4] I. M. Maafa *et al.*, “In Situ Preparation of 2D Co-B Nanosheets@1D TiO₂ Nanofibers as a Catalyst for Hydrogen Production from Sodium Borohydride,” *Inorganics*, vol. 11, no. 8, pp. 1–12, 2023, doi: 10.3390/inorganics11080342.
- [5] J. Ren, Z. Xia, B. Luo, D. Li, and W. Shi, “Fabrication of 2D/2D COF/SnNb₂O₆ nanosheets and their enhanced solar hydrogen production,” *Inorganic Chemistry Frontiers*, vol. 8, no. 7, pp. 1686–1694, 2021, doi: 10.1039/D0QI01443E.
- [6] A. Sathyaseelan, K. Krishnamoorthy, P. Pazhamalai, N. U. H. L. Ali, and S. J. Kim, “Value-added methanol electroreforming coupled with green hydrogen production at the edge interface of 2D boron nanosheets,” *Journal of Materials Chemistry A*, vol. 11, no. 38, pp. 20712–20723, 2023, doi: 10.1039/d3ta03513a.
- [7] L. Wei *et al.*, “NiO Nanosheets Coupled with CdS Nanorods as 2D/1D Heterojunction for Improved Photocatalytic Hydrogen Evolution,” *Frontiers in Chemistry*, vol. 9, p. 655583, 2021, doi: 10.3389/fchem.2021.655583.
- [8] W. Xiong *et al.*, “Photocatalytic activity of 2D nanosheets of ferroelectric Dion-Jacobson compounds,” *Journal of Materials Chemistry A*, vol. 8, no. 14, pp. 6564–6568, 2020, doi: 10.1039/c9ta11639g.
- [9] K. C. Chong, C. Li, and B. Liu, “Recent Advances in Organic Photocatalysts for Solar Water Splitting,” *CCS Chemistry*, vol. 5, no. 11, pp. 2436–2447, 2023, doi: 10.31635/ccschem.023.202302868.
- [10] H. Fu *et al.*, “A scalable solar-driven photocatalytic system for separated H₂ and O₂ production from water,” *Nature Communications*, vol. 16, no. 1, pp. 1–12, 2025, doi: 10.1038/s41467-025-56314-x.
- [11] I. Hong, Y. A. Chen, Y. J. Hsu, and K. Yong, “Triple-channel charge transfer over w18o49/au/g-c3n4 z-scheme photocatalysts for achieving broad-spectrum solar hydrogen production,” *ACS Applied Materials and Interfaces*, vol. 13, no. 44, pp. 52670–52680, 2021, doi: 10.1021/acsami.1c15883.
- [12] A. Murali, R. S. Singh, M. L. Free, and P. K. Sarswat, “Enhanced interfacial charge transfer by Z-scheme in defect-mediated ZnO-CdS nano-composite with rGO as a solid-state electron mediator for efficient photocatalytic applications,” *arXiv preprint*, 2023, doi: 10.48550/arXiv.2308.05211.
- [13] K. Murofushi *et al.*, “Earth-abundant iron (iii) species serves as a cocatalyst boosting the multielectron reduction of IO₃-I-redox shuttle in Z-scheme photocatalytic water splitting,” *Journal of Materials Chemistry A*, vol. 9, no. 19, pp. 11718–11725, 2021, doi: 10.1039/dlta01703a.
- [14] L. Schumacher and R. Marschall, “Recent Advances in Semiconductor Heterojunctions and Z-Schemes for Photocatalytic Hydrogen Generation,” *Topics in Current Chemistry*, vol. 380, no. 6, pp. 1–42, 2022, doi: 10.1007/s41061-022-00406-5.
- [15] T. L. Wakjira, A. B. Gemta, G. B. Kassahun, D. M. Andoshe, and K. Tadele, “Bismuth-Based Z-Scheme Heterojunction Photocatalysts for Remediation of Contaminated Water,” *ACS Omega*, vol. 9, no. 8, pp. 8709–8729, 2024, doi: 10.1021/acsomega.3c08939.
- [16] J. Wang *et al.*, “Two-dimensional graphitic carbon nitride/N-doped carbon with a direct Z-scheme heterojunction for photocatalytic generation of hydrogen,” *Nanoscale Advances*, vol. 3, no. 23, pp. 6580–6586, 2021, doi: 10.1039/d1na00629k.
- [17] H. Fu *et al.*, “Photocatalytic Overall Water Splitting with a Solar-to-Hydrogen Conversion Efficiency Exceeding 2 % through Halide Perovskite,” *Angewandte Chemie - International Edition*, vol. 63, no. 49, 2024, doi: 10.1002/anie.202411016.
- [18] D. Gunawan *et al.*, “Materials Advances in Photocatalytic Solar Hydrogen Production: Integrating Systems and Economics for a Sustainable Future,” *Advanced Materials*, vol. 36, no. 42, pp. 1–37, 2024, doi: 10.1002/adma.202404618.
- [19] Hydrogen Newsletter, “Photocatalytic Water Splitting for Hydrogen Production: Principles, Advances, and Future Directions,” www.hydrogennewsletter.com. [Online]. Available: <https://www.hydrogennewsletter.com/photocatalytic-water-splitting-for-hydrogen-production-principles-advances-and-future-directions/> (Accessed: Mar. 09, 2025).
- [20] M. Kumar, N. K. Singh, R. S. Kumar, and R. Singh, “Production of Green Hydrogen through Photocatalysis,” *ACS Symposium Series*, vol. 1468, pp. 1–24, 2024, doi: 10.1021/bk-2024-1468.ch001.
- [21] T.-H. Lin, Y.-H. Chang, K.-P. Chiang, J.-C. Wang, and M.-C. Wu, “Nanoscale Multidimensional Pd/TiO₂/g-C₃N₄ Catalyst for Efficient Solar-Driven Photocatalytic Hydrogen Production,” *Catalysts*, vol. 11, no. 1, p. 59, Jan. 2021, doi: 10.3390/catal11010059.
- [22] S. S. Mani, S. Rajendran, T. Mathew, and C. S. Gopinath, “A review on the recent advances in the design and structure-activity relationship of TiO₂-based photocatalysts for solar hydrogen production,” *Energy Advances*, vol. 3, no. 7, pp. 1472–1504, 2024, doi: 10.1039/d4ya00249k.
- [23] C. McFadden, “Japan: Scientists develop new tech to turn sunlight, water into hydrogen fuel,” interestingengineering.com. [Online]. Available: <https://interestingengineering.com/energy/japan-sunlight-powered-hydrogen-production> (Accessed: Dec. 03, 2024).
- [24] M. Mohsin *et al.*, “Semiconductor Nanomaterial Photocatalysts for Water-Splitting Hydrogen Production: The Holy Grail of Converting Solar Energy to Fuel,” *Nanomaterials*, vol. 13, no. 3, p. 546, 2023, doi: 10.3390/nano13030546.
- [25] M. Rafique *et al.*, “Hydrogen Production Using TiO₂-Based Photocatalysts: A Comprehensive Review,” *ACS Omega*, vol. 8, no. 29, pp. 25640–25648, 2023, doi: 10.1021/acsomega.3c00963.
- [26] M. M. Rana, F. A. Rafi, B. Agili, and A. S. A. Shahranj, “Advancements in Green Hydrogen Production from Photocatalytic Seawater Splitting,” *European Journal of Electrical Engineering and Computer Science*, vol. 8, no. 2, pp. 1–8, 2024, doi: 10.24018/ejece.2024.8.2.616.
- [27] P. Ravi and J. Noh, “Photocatalytic Water Splitting: How Far Away Are We from Being Able to Industrially Produce Solar Hydrogen?,” *Molecules*, vol. 27, no. 21, pp. 1–25, 2022, doi: 10.3390/molecules27217176.
- [28] M. K. Son, “Recent Research Progresses and Challenges for Practical Application of Large-Scale Solar Hydrogen Production,” *Molecules*, vol. 29, no. 24, p. 6003, 2024, doi: 10.3390/molecules29246003.
- [29] H. Song, S. Luo, H. Huang, B. Deng, and J. Ye, “Solar-Driven Hydrogen Production: Recent Advances, Challenges, and Future Perspectives,” *ACS Energy Letters*, vol. 7, no. 3, pp. 1043–1065, 2022.
- [30] X. Tao, Y. Zhao, S. Wang, C. Li, and R. Li, “Recent advances and perspectives for solar-driven water splitting using particulate photocatalysts,” *Chemical Society Reviews*, vol. 51, no. 9, pp. 3561–3608, 2022, doi: 10.1039/d1cs01182k.
- [31] A. Wawrzynczak and A. Feliczkak-Guzik, “Hydrogen Production Using Modern Photocatalysts,” *Coatings*, vol. 14, no. 3, p. 366, 2024, doi: 10.3390/coatings14030366.

[32] P. Zhou *et al.*, "Solar-to-hydrogen efficiency of more than 9% in photocatalytic water splitting," *Nature*, vol. 613, no. 7942, pp. 66–70, 2023, doi: 10.1038/s41586-022-05399-1.

[33] N. Baig, I. Kammakakam, W. Falath, and I. Kammakakam, "Nanomaterials: A review of synthesis methods, properties, recent progress, and challenges," *Materials Advances*, vol. 2, no. 6, pp. 1821–1871, 2021, doi: 10.1039/d0ma00807a.

[34] B. Cho and Y. Kim, "Preparation and properties of 2D materials," *Nanomaterials*, vol. 10, no. 4, p. 764, 2020, doi: 10.3390/nano10040764.

[35] I. Cho, J. Ko, D. D. O. Henriquez, D. Yang, and I. Park, "Recent Advances in 1D Nanostructure Assembly and Direct Integration Methods for Device Applications," *Small Methods*, vol. 8, no. 12, pp. 1–30, 2024, doi: 10.1002/smtd.202400474.

[36] X. Du *et al.*, "Bifunctionally faceted Pt/Ru nanoparticles for preferential oxidation of CO in H₂," *Journal of Catalysis*, vol. 396, pp. 148–156, 2021, doi: 10.1016/j.jcat.2021.02.010.

[37] J. Fatima *et al.*, "Tunable 2D Nanomaterials: Their Key Roles and Mechanisms in Water Purification and Monitoring," *Frontiers in Environmental Science*, vol. 10, pp. 1–23, 2022, doi: 10.3389/fenvs.2022.766743.

[38] J. Fonseca and J. Lu, "Single-Atom Catalysts Designed and Prepared by the Atomic Layer Deposition Technique," *ACS Catalysis*, vol. 11, no. 12, pp. 7018–7059, 2021, doi: 10.1021/acscatal.1c01200.

[39] Y.-T. Guo and S.-S. Yi, "Recent Advances in the Preparation and Application of Two-Dimensional Nanomaterials," *Materials*, vol. 16, no. 17, p. 5798, Aug. 2023, doi: 10.3390/ma16175798.

[40] V. Harish *et al.*, "Nanoparticle and Nanostructure Synthesis and Controlled Growth Methods," *Nanomaterials*, vol. 12, no. 18, pp. 1–30, 2022, doi: 10.3390/nano12183226.

[41] S. Hettler, M. Furqan, and R. Arenal, "Support-Based Transfer and Contacting of Individual Nanomaterials for In Situ Nanoscale Investigations," *Small Methods*, vol. 8, no. 12, pp. 1–13, 2024, doi: 10.1002/smtd.202400034.

[42] R. Li *et al.*, "Aquatic environment remediation by atomic layer deposition-based multi-functional materials: A review," *Journal of Hazardous Materials*, vol. 402, p. 123513, 2021, doi: 10.1016/j.jhazmat.2020.123513.

[43] Y. Liu, Y. Wang, and N. Pinna, "Atomically Precise Metal Nanoclusters for Photocatalytic Water Splitting," *ACS Materials Letters*, vol. 6, no. 7, pp. 2995–3006, 2024, doi: 10.1021/acsmaterialslett.4c00622.

[44] J. Lu, "A Perspective on New Opportunities in Atom-by-Atom Synthesis of Heterogeneous Catalysts Using Atomic Layer Deposition," *Catalysis Letters*, vol. 151, no. 6, pp. 1535–1545, 2021, doi: 10.1007/s10562-020-03412-8.

[45] A. Machin *et al.*, "One-dimensional (1d) nanostructured materials for energy applications," *Materials*, vol. 14, no. 10, p. 2609, 2021, doi: 10.3390/ma14102609.

[46] F. Naeem *et al.*, "Atomic layer deposition synthesized ZnO nanomembranes: A facile route towards stable supercapacitor electrode for high capacitance," *Journal of Power Sources*, vol. 451, p. 227740, 2020, doi: 10.1016/j.jpowsour.2020.227740.

[47] NOTE-01, "Nanotechnology Introduction: A Complete Beginner's Guide," www.nanowerk.com. [Online]. Available: https://www.nanowerk.com/nanotechnology/introduction/introduction_to_nanotechnology_1.php (Accessed: Jun. 01, 2025).

[48] NOTE-02, "One-dimensional (1D) materials," www.nanowerk.com. [Online]. Available: <https://www.nanowerk.com/1D-materials.php> (Accessed: Jun. 01, 2025).

[49] G. Paramasivam, V. V. Palem, T. Sundaram, V. Sundaram, S. C. Kishore, and S. Bellucci, "Nanomaterials: Synthesis and applications in theranostics," *Nanomaterials*, vol. 11, no. 12, p. 3228, 2021, doi: 10.3390/nano11123228.

[50] L. Peng *et al.*, "One-dimensionally oriented self-assembly of ordered mesoporous nanofibers featuring tailorable mesophases via kinetic control," *Nature Communications*, vol. 14, no. 1, p. 8148, 2023, doi: 10.1038/s41467-023-43963-z.

[51] J. Restivo, O. S. G. P. Soares, and M. F. R. Pereira, "Processing methods used in the fabrication of macrostructures containing 1d carbon nanomaterials for catalysis," *Processes*, vol. 8, no. 11, pp. 1–36, 2020, doi: 10.3390/pr8111329.

[52] H. M. Saleh and A. I. Hassan, "Synthesis and Characterization of Nanomaterials for Application in Cost-Effective Electrochemical Devices," *Sustainability*, vol. 15, no. 14, p. 10891, 2023, doi: 10.3390/su151410891.

[53] V. Shanmugam *et al.*, "A Review of the Synthesis, Properties, and Applications of 2D Materials," *Particle and Particle Systems Characterization*, vol. 39, no. 6, p. 2200031, 2022, doi: 10.1002/ppsc.202200031.

[54] Paras *et al.*, "A Review on Low-Dimensional Nanomaterials: Nanofabrication, Characterization and Applications," *Nanomaterials*, vol. 13, no. 1, p. 160, 2023, doi: 10.3390/nano13010160.

[55] F. Yang *et al.*, "Tuning Internal Strain in Metal–Organic Frameworks via Vapor Phase Infiltration for CO₂ Reduction," *Angewandte Chemie - International Edition*, vol. 59, no. 11, pp. 4572–4580, 2020, doi: 10.1002/anie.202000022.

[56] J. Yang, K. Cao, M. Gong, B. Shan, and R. Chen, "Atomically decorating of MnO_x on palladium nanoparticles towards selective oxidation of benzyl alcohol with high yield," *Journal of Catalysis*, vol. 386, pp. 60–69, 2020, doi: 10.1016/j.jcat.2020.03.029.

[57] F. Yang *et al.*, "Design of active and stable oxygen reduction reaction catalysts by embedding Co_xO_y nanoparticles into nitrogen-doped carbon," *Nano Research*, vol. 10, no. 1, pp. 97–107, 2017, doi: 10.1007/s12274-016-1269-5.

[58] S. Yuan and Q. Zhang, "Application of One-Dimensional Nanomaterials in Catalysis at the Single-Molecule and Single-Particle Scale," *Frontiers in Chemistry*, vol. 9, pp. 1–6, Dec. 2021, doi: 10.3389/fchem.2021.812287.

[59] J. Zhang, Y. Li, K. Cao, and R. Chen, "Advances in Atomic Layer Deposition," *Nanomanufacturing and Metrology*, vol. 5, no. 3, pp. 191–208, 2022, doi: 10.1007/s41871-022-00136-8.

[60] D. Zheng, Y. Xue, J. Wang, P. S. Varbanov, J. J. Klemeš, and C. Yin, "Nanocatalysts in photocatalytic water splitting for green hydrogen generation: Challenges and opportunities," *Journal of Cleaner Production*, vol. 414, p. 137700, 2023, doi: 10.1016/j.jclepro.2023.137700.

[61] J. Wang *et al.*, "Precise control of TiO₂ overlayer on hematite nanorod arrays by ALD for the photoelectrochemical water splitting," *Sustainable Energy and Fuels*, vol. 8, no. 16, pp. 3753–3763, 2024, doi: 10.1039/d3se01633a.

[62] T. R. Harris-Lee, A. Brookes, J. Zhang, C. L. Bentley, F. Marken, and A. L. Johnson, "Plasma-Enhanced Atomic Layer Deposition of Hematite for Photoelectrochemical Water Splitting Applications," *Crystals*, vol. 14, no. 8, p. 723, 2024, doi: 10.3390/cryst14080723.

[63] J. Kwon, S. Ko, H. Kim, H. J. Park, C. Lee, and J. Yeo, "Recent advances in vacuum- and laser-based fabrication processes for solar water-splitting cells," *Materials Chemistry Frontiers*, vol. 8, no. 11, pp. 2322–2340, 2024, doi: 10.1039/d3qm01336g.